

Numerical Study of the Roberge-Weiss Transition.

V. G. Bornyakov

*Institute for High Energy Physics NRC “Kurchatov Institute”, 142281 Protvino, Russia
Institute of Theoretical and Experimental Physics NRC “Kurchatov Institute”, 117218 Moscow, Russia*

N. V. Gerasimeniuk, V. A. Goy, A. A. Korneev, and A. V. Molochkov
Pacific Quantum Center, Far Eastern Federal University, 690950 Vladivostok, Russia

A. Nakamura

*RCNP, Osaka University, Osaka 567-0047, Japan and
Pacific Quantum Center, Far Eastern Federal University, 690950 Vladivostok, Russia*

R. N. Rogalyov

*Institute for High Energy Physics NRC “Kurchatov Institute”,
142281 Protvino, Russia*

We study numerically the Roberge-Weiss (RW) phase transition associated with the discontinuities in the quark-number density at a definite series of the values of the imaginary part of the quark chemical potential. We use polynomial fit functions to parametrize the quark number density, ρ , for computing the canonical partition functions and show that they provide a good framework for the analysis of lattice QCD data at finite density and $T > T_{RW}$. We argue that at high temperatures the Lee-Yang zeroes (LYZ) lie in the negative real semiaxis provided that the high-quark-number contributions to the great canonical partition function do not vanish. Nonzero linear density of the LYZ distribution signals the RW phase transition.

PACS numbers: 11.15.Ha, 12.38.Gc, 12.38.Aw

Keywords: Quantum chromodynamics, Lee-Yang zeros, Roberge-Weiss transition

I. INTRODUCTION

Properties of strong-interacting matter at nonzero temperature T and quark chemical potential μ_q have received considerable attention. QCD phase diagram in the $T - \mu_q$ plane is expected to have a rich structure, which can be studied experimentally in high-energy nuclear collisions and astronomical observations of the neutron stars. For many years, it had been thought that the lattice-QCD studies of strong-interacting matter at finite T and μ_q is impossible because of the sign problem. And yet, thanks to recent developments, now we can access the regions at finite T and μ_q up to $\mu_q/T \sim 1$.

When the chemical potential is pure imaginary, $\mu_q = i\mu_{qI}$, there is no sign problem. Therefore, we can evaluate various quantities by the Monte Carlo simulations. Especially if the partition functions, Z_C are obtained, the grand partition function, Z_{GC} , is available at both real and imaginary chemical potential because of the following fugacity expansion

$$Z_{GC}(\mu, T, V) = \sum_{n=-\infty}^{\infty} Z_C(n, T) \xi_B^n, \quad (1)$$

i.e., QCD at the real μ_q is determined at the pure chemical potential regions. We call it the canonical approach.

The first-order RW phase transition [1] was investigated in lattice QCD [2]. There exist lattice results and phenomenological models for the Fourier coefficients [4]. Computation of Z_n and LYZ for these models can bring more understanding and is our next task. Independent models for Z_n will be also useful for understanding QCD phase structure at finite temperature and quark density. In this paper we make a first step in this direction. Namely, we construct Z_n at high temperature above the Roberge-Weiss transition temperature T_{RW} where the quark number density lattice results can be described by a polynomial function of the quark chemical potential. We show that our approximate solution for Z_n becomes exact in the infinite volume limit. Then we use obtained Z_n to compute the Lee-Yang zeros (LYZ) and show that all LYZ are on the negative real axes in the complex fugacity ξ plain. Nonzero linear density of LYZ at $\xi = -1$ corresponding to RW transition is reached in the infinite-volume limit.

The paper is organized as follows. In Section II we describe numerical procedure of determination of the canonical partition functions as well as their asymptotic estimate based on the use of the polynomial fit to

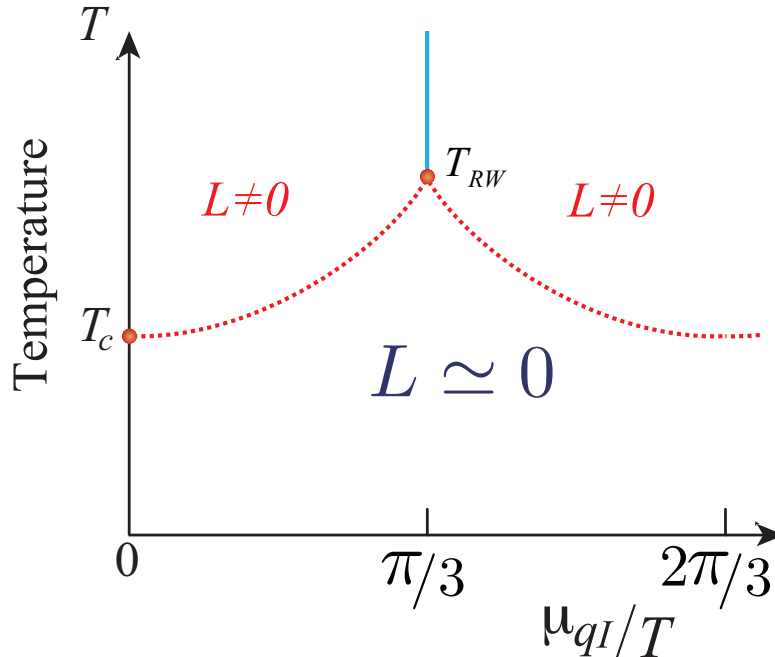


FIG. 1: Schematic figure of Roberge-Weiss phase structure at $\mu_q = i\mu_{qI}$. T_c is the confinement/deconfinement crossover point at zero chemical potential, L is the Polyakov loop. The vertical line ($T \geq T_{RW}$, $\mu_I/T = \pi/3$) shows the first order phase transition. The dashed line is a crossover where the first order phase transition for large or small quark masses.

our lattice data on the quark density. In Section III we compute the LYZ and discuss the pattern of their distribution in the fugacity plane. The obtained results are summarized in the Conclusions.

By studying QCD at imaginary chemical potential, one can gain understanding not only of the Roberge-Weiss transition but also of the critical properties of QCD related to deconfinement, chiral symmetry restoration and critical endpoint [13].

II. COMPUTATION OF THE CANONICAL PARTITION FUNCTIONS

In the following, we abbreviate the normalized canonical partition function, $Z_C(n, T, V)/Z_C(0, T, V)$, as Z_n . It was observed that at imaginary $\mu_q = i\mu_{qI}$, the quark number density (which is also imaginary, $\rho = i\rho_I$) can be well approximated by an odd power polynomial at high temperatures above the Roberge-Weiss transition temperature T_{RW} , and by the Fourier series at lower temperatures [3, 5–9].

In Ref. [3] we developed a method to compute Z_n numerically which is to fit the lattice data for the quark number density ρ_I to some function (thus determining $Z_{GC}(\theta, T, V)$ up to a factor) and to complete the Fourier transformation numerically

$$Z_n = \int_0^{2\pi} \frac{d\theta}{2\pi} e^{-in\theta} Z_{GC}(\theta, T, V), \quad (2)$$

where $\theta = \mu_I/T$. It was found [3, 7] that at $T > T_{RW}$, i.e. above the Roberge-Weiss transition, one can fit the lattice data for the quark number density, which is a periodic function with period $2\pi/3$, by the function

$$\hat{\rho} = a_1\theta - a_3\theta^3 + a_5\theta^5, \quad -\pi/3 < \theta < \pi/3, \quad a_i > 0 \quad (3)$$

where $\hat{\rho} = \rho_I/T^3$.

Using this form of the number density we computed Z_n at $T > T_{RW}$ for n up to some n_{max} [3]. For $n > n_{max}$ Z_n computed via eq. (2) has alternating sign which is unphysical and signals that our fit-function is not suitable. n_{max} depends on volume while the corresponding (dimensionless) density $\hat{\rho}_{max} = n_{max}/(VT^3)$ is only weakly dependent on volume is approximately equal to 4.83 for $T/T_c = 1.35$.

The reason for such unphysical behavior of Z_n (note that Z_n is to be positive) is that eq. (3) imposes unphysical condition of a phase transition onto our finite-volume system. Indeed, the function defined by eq. (3) is discontinuous at $\theta = \pi/3 + 2\pi k/3$, $k = \pm 1, \pm 2, \dots$. Note that with $Z_n, n < n_{max}$ obtained in [3] we are able to reproduce the number density $\hat{\rho}$ dependence on theta for all θ apart from the vicinity of $\theta_I = \pi/3$.

Thus we have to modify the right-hand side of eq. (3) in the vicinity of the Roberge-Weiss transition. This modification should be volume dependent and show the discontinuous behavior eq. (3) only in the infinite volume limit. To compute the quark number density ρ_I in the close vicinity of the transition point $\theta_I = \pi/3$ is a formidable task. We follow another strategy and use an approximate analytical solution for Z_n originally suggested in [1]. In this study, we considerably improve the approximation suggested in [1] and demonstrate that this improved approximation has necessary behavior near $\theta_I = \pi/3$ and reproduces density (3) in the infinite volume limit.

Roberge and Weiss [1] obtained an approximate expression for Z_n in the case when $a_5 = 0$. They computed the integral

$$Z_{nA} = \frac{\int_0^{\pi/3} d\theta e^{-F_n(\theta)}}{\int_0^{\pi/3} d\theta e^{-F_0(\theta)}} \quad (4)$$

where

$$F_n(\theta) = -(in\theta - VT^3(\frac{1}{2}a_1\theta^2 - \frac{1}{4}a_3\theta^4)) \quad (5)$$

using the stationary phase method. It is reasonable to apply the method in the $V \rightarrow \infty$ limit. The stationary condition is

$$in - VT^3(a_1\theta - a_3\theta^3) = 0 \quad (6)$$

with solution $\theta = i\hat{\mu}_0(\hat{\rho}), \hat{\mu}_0(\hat{\rho})$:

$$a_3\hat{\mu}_0^3 + a_1\hat{\mu}_0 - \hat{\rho} = 0. \quad (7)$$

This equation can be solved by radicals:

$$\hat{\mu}_0 = \sqrt{\frac{a_1}{3a_3}} \left[(\sqrt{x^2 + 1} + x)^{1/3} - (\sqrt{x^2 + 1} - x)^{1/3} \right], \quad (8)$$

where $x = \hat{\rho} \frac{\sqrt{27a_3}}{2a_1^{3/2}}$. Then the approximate expression obtained in [1] is

$$Z_{nA}/Z_{0A} = \frac{e^{-F_n(\hat{\mu}_0)}}{e^{-F_0(\hat{\mu}_0)}} \quad \text{where} \quad F_n(\hat{\mu}_0) = -VT^3 \frac{1}{4} (a_1\hat{\mu}_0^2 - 3\hat{\rho}\hat{\mu}_0), \quad (9)$$

where $\hat{\mu}_0$ is found from eq. (7).

Thus the canonical partition functions Z_n can be computed both by the asymptotic formula (9) and by formula (2) numerically. The canonical partition functions Z_n determined by the former procedure are denoted Z_{nA} , by the latter — Z_{nN} . The values of Z_{nN} were computed in [3] using the quark density obtained in numerical simulations at $T/T_c = 1.35$ on lattices 4×16^3 . These values and the values of Z_{nA} computed for the respective constants a_1, a_3 are shown in Fig. 2. One can see that they agree for $n < n_{max}$. At $n > n_{max}$ Z_{nN} starts to oscillate as described above.

To compare Z_{nN} and Z_{nA} more explicitly we estimate the relative deviation

$$R = (Z_{nN} - Z_{nA})/Z_{nN}$$

for three volumes at $\hat{\rho} \leq 4.83$: at $\hat{\rho} < 1.5$ the relative deviation is rather small, ($R < 0.04$), but it increases rather fast reaching 0.2 at the maximal $\hat{\rho}$ for which Z_{nN} is available. We shall note that the numerical values for a_1 and a_3 were obtained on $V = 16^3$ lattices. In what follows we use same values for all volumes assuming very weak volume dependence of a_i . This is supported by our numerical results [3] on volume dependence of a_i .

In fact the expression (9) is not the full story. One can take into account the fluctuations around $\hat{\mu}_0$ to obtain

$$Z_{nA}/Z_{0A} = \frac{e^{-F_n(\hat{\mu}_0)}}{e^{-F_0(\hat{\mu}_0)}} \frac{\sqrt{F_0''(\hat{\mu}_0)}}{\sqrt{F_n''(\hat{\mu}_0)}} \quad (10)$$

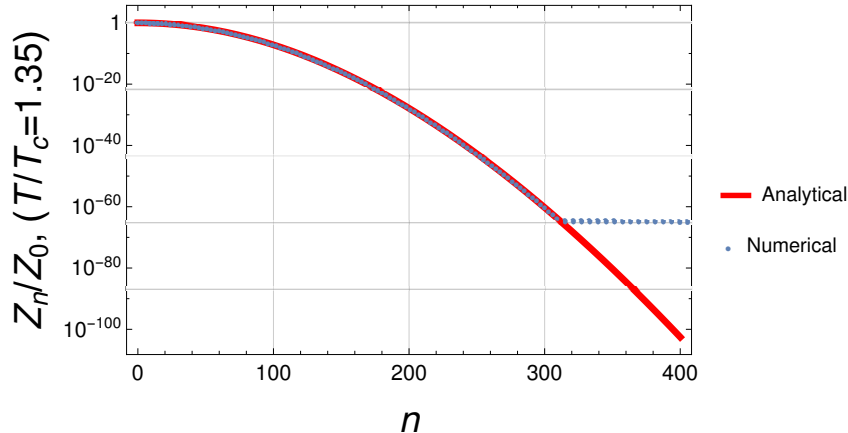


FIG. 2: Z_{nN}/Z_{0N} at $T/T_c = 1.35$ (red line) are compared with Z_{nA}/Z_{0A} (blue dots). At $n > 309$ only the absolute value of Z_{nN}/Z_{0N} is shown.

where

$$F_n''(\hat{\mu}_0) = VT^3(a_1 + 3a_3\hat{\mu}_0^2) \quad (11)$$

Our result eq. (10) is much closer to Z_{nN} than the result eq. (9) obtained in [1]. R goes to zero in the infinite volume limit for all values of density $\hat{\rho}_q$ under consideration.

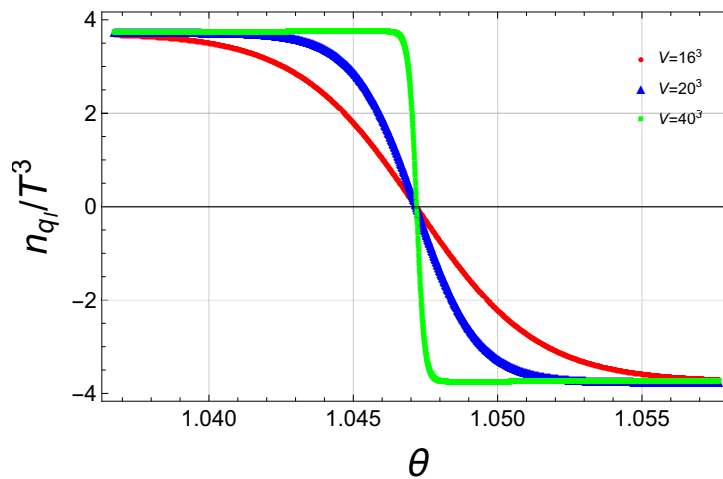


FIG. 3: The quark number density computed using Z_{nA} at $T/T_c = 1.35$ for imaginary chemical potential for three volumes and $\rho = \rho_{max}$ over a restricted range near $\pi/3$.

Another way to check the quality of the obtained approximation for Z_n is to compute the quark number density using Z_{nA} and compare it with the number density we used as the input (3). In Fig. 3(right) we show the quark number density $\hat{\rho}_{qI}$ computed via Z_{nA} in the vicinity of the critical value $\theta = \pi/3$. The volume dependence of the density becomes visible: with increasing volume the number density approaches a step function, i.e. the first order phase transition appears in the infinite volume limit.

The relative deviation for the quark number density is shown in Fig. 4 for three spatial volumes. In the left panel it is shown for imaginary μ . The deviation is small and shows very fast decreasing with increasing V . Note that the relative deviation increases near $\hat{\mu} = \pi/3$ since eq. (3) gives a correct number density in this range in the infinite volume limit only. In the right panel we show the relative deviation for the real chemical potential. Again we see that this relative deviation is small and decreases with an increase of the volume.

For $a_5 \neq 0$, an explicit solution of eq. (3) is not available. However, considering a_5 as a small parameter we obtained an approximate solution up to order a_5^2 :

$$\hat{\mu} = \hat{\mu}_0 + a_5 \hat{\mu}_1 + a_5^2 \hat{\mu}_2, \quad (12)$$

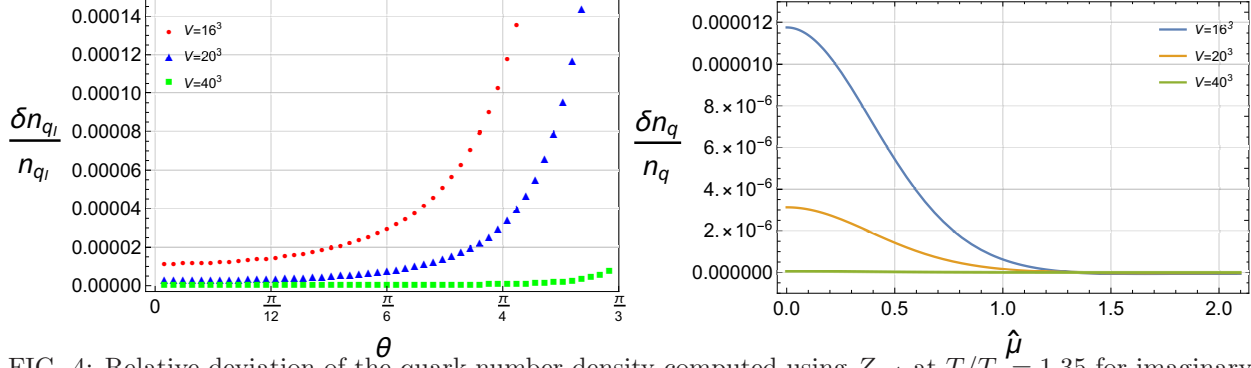


FIG. 4: Relative deviation of the quark number density computed using Z_{nA} at $T/T_c = 1.35$ for imaginary chemical potential (left panel) and the real chemical potential (right panel).

where

$$\hat{\mu}_1 = -\frac{\hat{\mu}_0^5}{a_1 + 3a_3\hat{\mu}_0^2} \quad (13)$$

$$\hat{\mu}_2 = -\frac{5\hat{\mu}_1\hat{\mu}_0^4 + 3a_3\hat{\mu}_1^2\hat{\mu}_0}{a_1 + 3a_3\hat{\mu}_0^2} \quad (14)$$

Then, following procedure described in eqs. (4-10) we find

$$Z_{nA}/Z_0 = \frac{e^{-F_n(\hat{\mu})} \sqrt{F_0''(\hat{\mu})}}{e^{-F_0(\hat{\mu})} \sqrt{F_n''(\hat{\mu})}}, \quad (15)$$

where

$$F_n(\hat{\mu}) = -VT^3 \frac{1}{4} (a_1\hat{\mu}_0^2 - 3\hat{\rho}\hat{\mu}_0 + a_5f_1(\hat{\mu}_0) + a_5^2f_2(\hat{\mu}_0) + O(a_5^3)), \quad (16)$$

$$F_n''(\hat{\mu}) = VT^3 (a_1 + 3a_3\hat{\mu}_0^2 + a_5f_3(\hat{\mu}_0) + a_5^2f_4(\hat{\mu}_0) + O(a_5^3)), \quad (17)$$

$$f_1(\hat{\mu}_0) = \frac{2}{3}\hat{\mu}_0^6 \quad (18)$$

$$f_2(\hat{\mu}_0) = -\frac{2\hat{\mu}_0^{10}}{a_1 + 3a_3\hat{\mu}_0^2} \quad (19)$$

$$f_3(\hat{\mu}_0) = \hat{\mu}_0^4 \left(3 + \frac{2a_1}{a_1 + 3a_3\hat{\mu}_0^2} \right) \quad (20)$$

$$f_4(\hat{\mu}_0) = -\hat{\mu}_0^8 \frac{20a_1^2 + 87a_1a_3\hat{\mu}_0^2 + 99a_3^2\hat{\mu}_0^4}{(a_1 + 3a_3\hat{\mu}_0^2)^3}. \quad (21)$$

To compute Z_{nA} for $T/T_c = 1.20$ we use $a_1 = 4.409, a_3 = 1.032, a_5 = -0.165$ [3] in eq. (3). It should be noted that with this set of constants a_i is not applicable at large real chemical potential since the quark density becomes negative. To keep the density positive we should assume that the coefficient a_7 which was not determined in [3] is positive. Z_{nA} for $T/T_c = 1.20$ are compared with Z_{nN} in Fig. ???. Good qualitative agreement is seen for the full range of n where Z_{nN} are available. The relative deviation R is small for $\hat{\rho} < 0.04$ and decreases with increasing volume but it increases fast for larger $\hat{\rho}$ and shows no decreasing with increasing volume. Respectively, we reproduce the quark number density dependence on $\hat{\mu}$ up to $\hat{\mu} < 2.0$ only.

III. EVALUATION OF LEE-YANG ZEROS

Lee-Yang zeros are zeros of the grand partition function $Z_{GC}(\mu_B, T, V)$, considered as a polynomial of the baryon fugacity $\xi_B = e^{\mu_B/T}$. In the finite volume V $Z_{GC}(\mu_B, T, V)$ has the form:

$$Z_{GC}(\mu_B, T, V) = \sum_{n=-n_{max}}^{n_{max}} Z_C(3n, T, V) \xi_B^n = e^{-n_{max} V \mu_B} \sum_{n=0}^{2n_{max}} Z_C(3n - n_{max}, T, V) \xi_B^n. \quad (22)$$

where $\mu_B = 3\mu_q$ is baryon chemical potential, $n_{max} = 2N_c N_f N_s^3 L_t$ for Wilson fermions. Computation of zeros of the high degree polynomial, eq.(22), is in general very difficult task. In this work we employ a very efficient package, MPSolve v.3.1.8 (Multiprecision Polynomial Solver) [10, 11], which provides calculation of polynomial roots with arbitrary precision.

In eq.(22) we rewrote $Z_{GC}(\mu_B, T, V)$ as a polynomial of degree $2n_{max}$ whose roots represent the values of the Lee-Yang zeros (LYZ) in the complex ξ_B -plane. Coefficients $Z_C(3n, T, V) \equiv Z_{3nA}$ are computed using eq.(10) with the GNU MPFR Library for multiple-precision floating-point computations. We performed calculations using the MPFR library with an accuracy from 1000 to 4000 digits. We found that 1000 digits is enough for MPSolve package to calculate LYZ for polynomial with degree less than 20,000. We also checked that to calculate LYZ for polynomials of degree greater than 30,000, it is necessary to use Z_{nA} calculated with an accuracy of more than 4,000 digits.

In practical lattice calculations at fixed lattice spacing a both $V/a^3 = N_s^3$ and the limits in the sum eq.(22) (which we denote as N_{max} in what follows) are finite. Thus we have to study dependence of the Lee-Yang zeros on N_{max} and N_s to make a conclusion about the infinite-volume limit. Analytical expression for the coefficients of the polynomial together with the use of MPSolve package allow us to work with an arbitrary degree of the polynomial limited only by the computational cost of LYZ calculation and to substantially improve our previous results [12] for $T > T_{RW}$. Our main goal is to understand the properties of LYZ in the vicinity of the Roberge-Weiss phase transition at $\xi_B = -1$.

In Fig.5 the results for LYZ are presented for three volumes with $N_s = 16, 20, 40$ and six values of N_{max} for each volume. These values of N_{max} change with volume and correspond to six volume independent values of the maximal quark number density $\hat{\rho}_{max} = N_{max}/(VT^3)$. We start with $\hat{\rho}_{max} = 3 \cdot 25/64 = 1.17$, and increase it up to $\hat{\rho}_{max} = 3 \cdot 205/64 = 9.61$.

In [12] it was found that the dependence on $\hat{\rho}_{max}$ is much more pronounced than the dependence on the volume. It was shown in [12] that for small $\hat{\rho}_{max}$ LYZ consist of two parts: the former part, P_1 , comprises the LYZ distributed along the unit circle $|\xi_B| = 1$ and the latter, P_2 , represents a curve starting on the circle at the end point of P_1 and extending towards the real positive axis. With increasing volume the endpoint of P_2 tends to approach the real axes.

It was demonstrated in [12] that P_1 shrinks to $\xi_B = -1$ with increasing $\hat{\rho}_{max}$. Respectively, one end of P_2 moves along the unit circle towards $\xi_B = -1$ while the other end slowly moves in the direction of $\xi_B = 0$. We now confirm these observations as can be seen from comparison of LYZ for $\hat{\rho}_{max} = 1.17, 2.24, 3.52, 4.69$ in Fig.5. But due to computations with much higher maximal density $\hat{\rho}_{max} = 5.02, 9.91$ we discover the correct properties of the LYZ in the limit $N_{max} \rightarrow n_{max}$.

In Fig.5 one can see that P_1 disappears completely at $\hat{\rho}_{max} > 4.7$. It is worth to note that this is approximately same value of the quark density which is reachable in computations of Z_{nN} .

The first real negative LYZ appears for $\hat{\rho}_{max} \approx 4.7$ for all volumes considered.

P_2 splits into two parts for $\hat{\rho}_{max} > 4.7$: P_{21} consisting of LYZ on the negative real axis $-1 < \xi_B < -\xi_{B0}$, $\xi_{B0} > 0$, with ξ_{B0} moving toward zero with increasing $\hat{\rho}_{max}$ and a curly part P_{22} connecting $-\xi_{B0}$ with the point slightly above the positive real axis. As we mentioned above, this point moves to the real axis in the infinite volume limit for fixed $\hat{\rho}_{max}$. When we first increase $\hat{\rho}_{max}$ to its maximal value for a given volume (in practical terms this implies the extrapolation to the infinite value) and then take the infinite volume limit we find that the right end of P_{22} goes to $\xi_B = 0$. We also find an indication that in the limit of infinite $\hat{\rho}_{max}$ $\xi_{B0} = 0$. We thus conclude that in the infinite volume limit all LYZ lie on the real negative axis.

Thus we see very strong dependence of LYZ on $\hat{\rho}_{max}$. It can be seen from Fig.5 that the finite volume effects are rather mild. For the maximal value of $\hat{\rho}_{max}$ shown in the figure one can see these effects in the enlarged insertion only.

Next we describe the properties of the LYZ on the real-negative axis. We found that for fixed volume they start to appear when N_{max} exceeds some value roughly equal $64 \cdot 4.7 \cdot N_s^3$. The LYZ most close to $\xi = -1$ appear first and with increasing N_{max} more and more remoted from -1 LYZ also appear. This property of LYZ can be seen in Fig.?? where we show the LYZ distribution for $N_s = 40$ in the complex chemical potential plain.

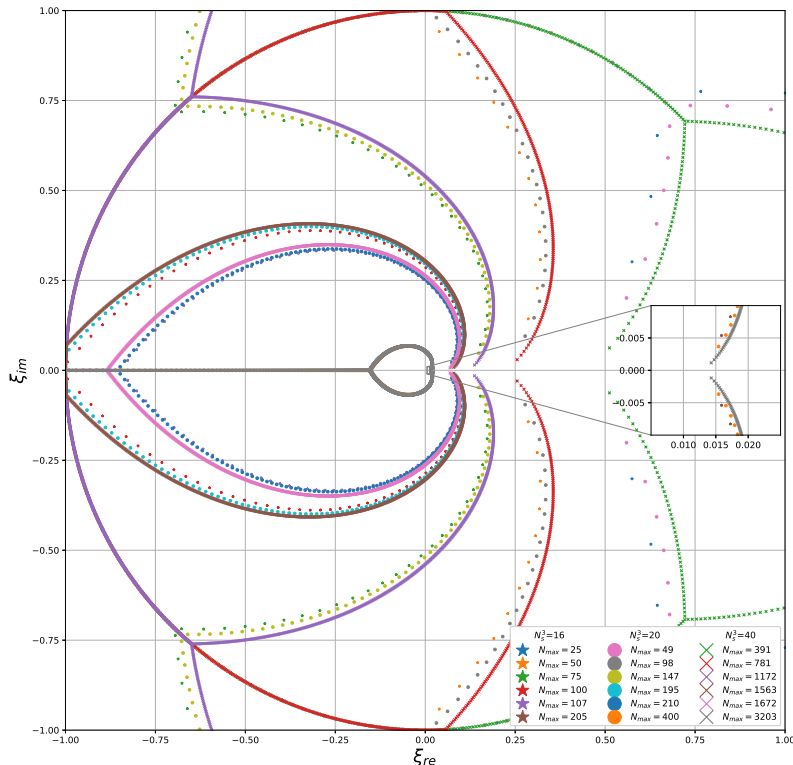


FIG. 5: LYZ distribution for $T/T_c = 1.35$

It is also seen that all LYZ on the real negative semiaxis lie equidistantly with distance roughly $d = 160/N_s^3$. Thus the linear density of LYZ remains finite in the infinite-volume limit. According to the criterion suggested in [14], the phase transition occurs at $Im(\mu) = \pi$.

IV. CONCLUSIONS

We studied $N_f = 2$ lattice QCD in the deconfinement phase above T_{RW} at $T/T_c = 1.35$. Our goal was to compute the distribution pattern of LYZ in the complex fugacity ξ_B plane and to demonstrate the existence of the LYZ close to $\xi = -1$ corresponding to the first order Roberge–Weiss transition at imaginary quark chemical potential.

In our earlier work [12] we have already made computations of LYZ at $T > T_{RW}$ using restricted number of Z_{nN} - canonical partition functions computed numerically via Fourier transformation. In this work, to overcome this restriction, we have used the approximate analytical expression Z_{nA} . We demonstrated that Z_{nA} agree very well with values of Z_{nN} where the latter are available and reproduce the input expression for the quark number density. In both cases the agreement improves with increasing volume.

Using Z_{nA} we were able to obtain correct behavior for the quark number density in the vicinity of the Roberge–Weiss phase transition at $\hat{\mu}_I = \pi/3$. We have demonstrated that, in the infinite volume limit, there appears a discontinuity in the dependence of $\hat{\rho}$ on $\hat{\mu}_I$ indicating the first-order transition behavior.

After we made sure that Z_{nA} works very well we computed the LYZ. Apart from increasing the available maximal density $\hat{\rho}_{max}$ which is now restricted only by the computation resources, we also used more effective procedure to compute LYZ. We used the effective MPSolve library with arbitrary precision. Our multi-precision computations were done with 4000 significant digits.

We confirmed our previous results obtained in [12] with restricted $\hat{\rho}_{max}$ about strong dependence of LYZ on

$\hat{\rho}_{max}$ and comparatively weak volume dependence.

Then, increasing $\hat{\rho}_{max}$, we discovered that the LYZ appear on the ξ negative real half-axis and in the infinite volume limit they fill in the full $Re(\xi) \leq 0$ range. This is in agreement with findings of [13]. We demonstrated that in the limit of large $\hat{\rho}_{max}$ there are no LYZ away from the ξ negative real axis. We have found that nonvanishing density of LYZ at $\xi = -1$ corresponding to the Roberge-Weiss first order phase transition at $T > T_{RW}$ and imaginary quark chemical potential appear only in the infinite volume limit.

Our result demonstrates necessity of using sufficiently high values of $\hat{\rho}_{max}$ to obtain correct results for LYZ. We believe that our results obtained in the of high temperatures where phase transitions are absent at real chemical potential will be useful for computation of LYZ at low temperature where phase transition or cross-over are present. This work is now under way.

Acknowledgments

This work was supported by the Russian Foundation for Basic Research via grant 18-02-40130 mega. Computer simulations were performed on the FEFU GPU cluster Vostok-1, the Central Linux Cluster of the NRC "Kurchatov Institute" - IHEP, the Linux Cluster of the NRC "Kurchatov Institute" - ITEP (Moscow). In addition, we used computer resources of the federal collective usage center Complex for Simulation and Data Processing for Mega-science Facilities at NRC Kurchatov Institute, <http://ckp.nrcki.ru/>.

-
- [1] A. Roberge and N. Weiss, Nucl. Phys. B275, 734, 1986.
 - [2] C. Bonati, G. Cossu, M. D'Elia and F. Sanfilippo, Phys. Rev. D **83** (2011), 054505 [arXiv:1011.4515 [hep-lat]].
 - [3] V.G.Bornyakov, D.L.Boyda, V.A.Goy, A.V.Molochkov, Atsushi Nakamura, A.A.Nikolaev, V.I. Zakharov Phys. Rev. **D95**, (2017) 094506.
 - [4] V. Vovchenko, J. Steinheimer, O. Philippsen and H. Stoecker, Phys. Rev. D **97** (2018) no.11, 114030, [arXiv:1711.01261 [hep-ph]].
 - [5] T. Takaishi, P. de Forcrand, A. Nakamura, PoS LAT 2009 (2009) 198, arXiv:1002.0890 [hep-lat].
 - [6] M. D'Elia, F. Sanfilippo, Phys. Rev. **D80** (2009) 014502, arXiv:0904.1400 [hep-lat].
 - [7] J. Takahashi, H. Kouno, M. Yahiro, Phys. Rev. **D91** (2015) 014501, arXiv:1410.7518 [hep-lat].
 - [8] M. D'Elia, G. Gagliardi, F. Sanfilippo, Phys. Rev. **D95** (2017) 094503, arXiv:1611.08285 [hep-lat].
 - [9] J. Gunther, R. Bellwied, S. Borsanyi, Z. Fodor, S.D. Katz, A. Pasztor, C. Ratti, EPJ Web Conf. 137 (2017) 07008, arXiv:1607.02493 [hep-lat].
 - [10] Bini, Dario A., Fiorentino, Giuseppe, Numerical Algorithms 23.2-3 (2000): 127-173.
 - [11] Bini, Dario A., and Robol, Leonardo. Journal of Computational and Applied Mathematics 272 (2014): 276-292.
 - [12] M. Wakayama, V. Bornyakov, D. Boyda, V. Goy, H. Iida, A. Molochkov, A. Nakamura and V. Zakharov, Phys. Lett. B **793**, 227-233 (2019) doi:10.1016/j.physletb.2019.04.040 [arXiv:1802.02014 [hep-lat]].
 - [13] G. A. Almasi, B. Friman, K. Morita, P. M. Lo and K. Redlich, Phys. Rev. D **100**, no.1, 016016 (2019) [arXiv:1805.04441 [hep-ph]].
 - [14] , T. D. Lee and Chen-Ning Yang, Phys. Rev. **87** (1952) pp. 410–419.